Chinese Chemical Letters 34 (2023) 108294

Contents lists available at ScienceDirect

Chinese Chemical Letters

journal homepage: www.elsevier.com/locate/cclet

Imidazobenzimidazole fused aza-calix[4]arenes: Synthesis, structure, and Zn^{2+}-selective colorimetric-fluorometric sensor

Yuan-Tao Huang[a], Min Xue[b], Yong Yang[a,*]

[a] Department of Chemistry, Key Laboratory of Surface & Interface Science of Polymer Materials of Zhejiang Province, Zhejiang Sci-Tech University, Hangzhou 310018, China
[b] Department of Physics, Key Laboratory of Optical Field Manipulation of Zhejiang Province, Zhejiang Sci-Tech University, Hangzhou 310018, China

ARTICLE INFO

Article history:
Received 21 November 2022
Revised 26 February 2023
Accepted 1 March 2023
Available online 5 March 2023

Keywords:
Aza-calix[4]arene
Imidazobenzimidazole
Fluorometric sensor
Zn^{2+}-selective

ABSTRACT

Tetra(amino)azacalix[4]arene skeleton was functionalized at the bridging NH sites using various aromatic aldehydes *via* formation of imidazobenzimidazole fused heterocycles. X-ray single crystal analysis revealed distorted 1,3-alternate conformations for the resulting macrocycles. Anthracenyl and pyrenyl modified imidazobenzimidazole fused aza-calix[4]arenes existed as dimers in the solid state, associated mainly through π-π stacking interactions between the planar polycyclic fluorophores. The tetrapyrenyl modified product was further used as a Zn^{2+}-selective sensor, which showed naked-eye detected color change and enhanced excimer emission. The stoichiometry between the sensor and Zn^{2+} was determined to be 1:1 and the association constant was 1.1×10^5 L/mol. The sensing process was highly selective and showed strong anti-interference with presence of other cations. The UV-vis spectral changes in the sensing process were completely reversible by alternate addition of Zn^{2+} and F^-, showing an efficient "on–off-on" result.

Calixarenes [1,2], a type of macrocycles with -CH_2- or -CHR- bridges linked at *meta* positions of aryls, have been prevailed in chemical community for nearly one century and in supramolecular chemistry for several decades. Replacing the bridging -CH_2- or -CHR- between aryls with other atoms such as oxygen, nitrogen, sulfur, silicon, the so called heterocalixarenes [3] or heterocalixaromatics [4] might be endowed with unique structures and fine tuning properties. Because of easy synthesis, thiacalixarenes are popular in supramolecular chemistry [5,6]. Oxa- [7,8] and aza-calixarenes [9,10], though reported several decades ago [11,12], did not invoke wide attention until synthesis breakthrough *via* nucleophilic aromatic substitution reaction (S_NAr) with mild reaction conditions, metal catalyst free and wide functional group tolerance by Wang [13] and Katz [14,15] in the early part of the 21st century. Unlike their calix[4]arene counterparts with various and flexible conformations, most oxa- and aza-calix[4]arenes adopted 1,3-alternate conformations both in solution and solid state, which greatly limited their applications. For example, great achievements were obtained in the field of fluorescent sensors with calixarenes [16,17]. However, there were only limited examples based on oxa- [18–21] and aza-calix[4]arenes [22]. Considering their easy synthesis, relatively fixed but still adjustable conformations, and facile installation of signal units and binding sites, oxa- and aza-calix[4]arenes might also serve as excellent platforms for this mission after suitable modification. This field is still underdeveloped and holds great potentials.

Usually, there are two ways of functionalization of aza-calix[4]arene skeletons: functionalizing the precursors for aza-calix[4]arene frameworks and post-macrocyclization derivation. Most post-macrocyclization derivation methods focused on the aromatic rings. Here we introduced a new strategy of derivation: functionalization at the bridging NH sites *via* formation of imidazobenzimidazole fused heterocycles. To the best of our knowledge, this is the first example of modification on the bridging NH sites.

Benzimidazoles and the relating imidazobenzimidazoles or benzobisimidazoles, are important heterocyclic pharmacophores [23–25]. They showed binding ability toward anions [26–28], cations [29,30], and DNA minor groove [31]. Here, we fused two imidazobenzimidazole motifs into an aza-calix[4]arene skeleton to integrate four N atoms on one rim, which we wished to capture metal cations *via* cooperative metal-ligand coordination interactions.

Recently, by installing four anthracenyls onto a tetra(amino)-oxacalix[4]arene framework with 1,3-alternate conformation *via*

* Corresponding author.
E-mail address: yangyong@zstu.edu.cn (Y. Yang).

https://doi.org/10.1016/j.cclet.2023.108294
1001-8417/

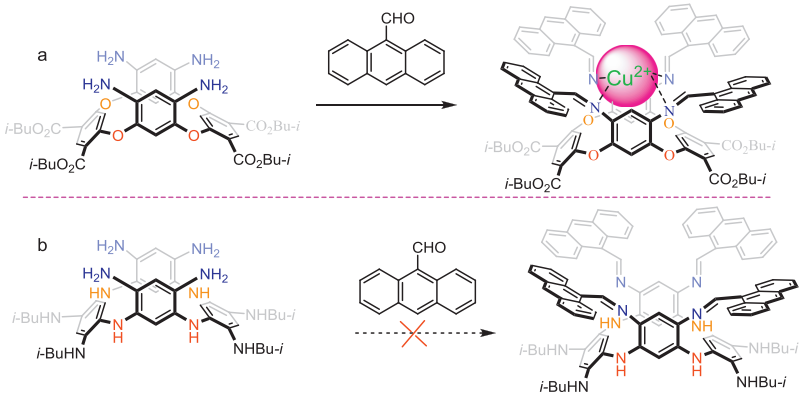

Scheme 1. (a) Synthesis of anthracenyl-modified oxa-calix[4]arene and illustration of Cu^{2+} sensing; (b) hypothesized anthracenyl-modified azacalix[4]arene.

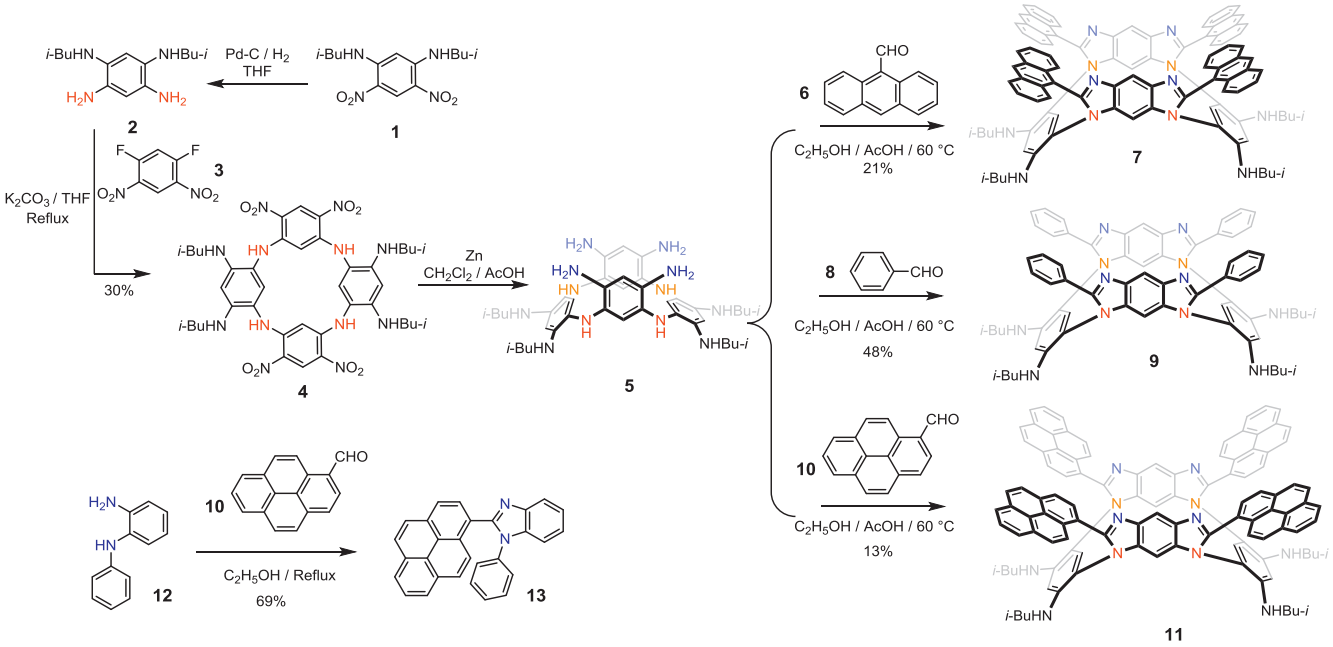

Scheme 2. Synthetic routes for the imidazobenzimidazole fused aza-calix[4]arenes **7**, **9**, **11**, and control compound **13**.

formation of four imine bonds to form a coordination pocket (Scheme 1a), we developed a colorimetric and "turn-on" fluorometric sensor for Cu^{2+} with high selectivity and strong anti-interference ability [32]. Similarly, we wished to functionalize a tetra(amino)azacalix[4]arene backbone *via* an analogous condensation reaction with anthracene-9-carbaldehyde to investigate the effect of different bridging atoms (Scheme 1b). Much to our surprise, we isolated an imidazobenzimidazole fused aza-calix[4]arene (Scheme 2), rather than the expected imine bonds linked product. The bridging NHs were involved in the reaction, which was confirmed *via* X-ray single crystal analysis (*vide infra*). With this finding in hand, we then attached pyrenyl fluorophores to this skeleton, which we wished to explore its cation selective sensing ability using fluorescence (FL) method. Due to its easy formation of an excimer emission band [33,34], pyrenyl was selected as a reporting unit for our fluorescent sensor.

The tetra(nitro)azacalix[4]arene skeleton was previously synthesized by Siri group *via* a fragment "3 + 1" strategy [35,36]. We tried a more efficient one-pot method. As shown in Scheme 2, N^1,N^3-diisobutyl-4,6-dinitrobenzene-1,3-diamine **1** was first reduced into N^1,N^5-diisobutylbenzene-1,2,4,5-tetraamine **2** under catalytic hydrogenation conditions, which was used without further purification and characterization. Then four folds of S_NAr reactions between equimolar amounts of compound **2** and 1,5-difluoro-2,4-dinitrobenzene **3** in refluxing THF using K_2CO_3 as a base afforded the symmetrically substituted aza-calix[4]arene **4** in 30% yield in a single step *via* a "2 + 2" manner. Only the primary amines were involved in this reaction and the secondary amines remained unchanged. The nitro groups on aza-calix[4]arene **4** were subsequently reduced again in the presence of Zn in CH_2Cl_2 and AcOH and the product was used without separation. Finally, the tetra(amino)azacalix[4]arene **5** condensed with four equivalents of anthracene-9-carbaldehyde **6** and then dehydroarylated using air as an oxidation reagent at 60 °C, affording the imidazobenzimidazole [25,37] fused aza-calix[4]arene **7** in 21% yield. This method proceeded smoothly also for benzaldehyde **8** and pyrene-1-carbaldehyde **10** to provide **9** (48%) and **11** (13%) over two steps, respectively. The relatively low yield might result from the strong oxidation propensity of the amines on **5**. Thus, four pyrenyl fluorophores were successfully attached to the aza-calix[4]arene skeleton at the bridging positions. The structures of the imidazobenzimidazole fused aza-calix[4]arenes **7**, **9**, and **11** were characterized thoroughly *via* ^{1}H NMR, ^{13}C NMR, high resolution mass spectroscopy, and X-ray single crystal analysis (only for **7** and **11**, *vide*

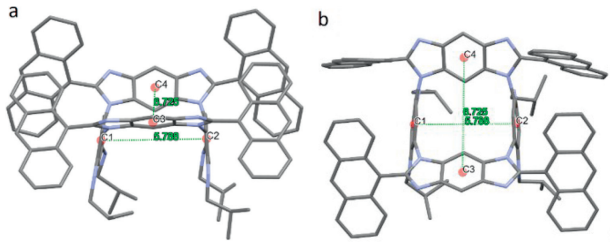

Fig. 1. X-ray single crystal structure of anthracenyl modified imidazobenzimidazole fused aza-calix[4]arene **7**: (a) side view; (b) top view. Hydrogen atoms are omitted for clarity.

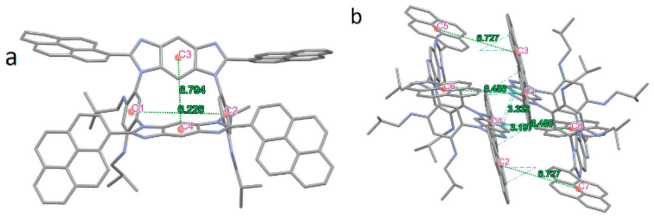

Fig. 2. X-ray single crystal structure of pyrenyl modified imidazobenzimidazole fused aza-calix[4]arene **11**: (a) side view; (b) illustration of intermolecular interactions in a dimer. Hydrogen atoms are omitted for clarity.

infra). Pyrenyl modified benzimidazole **13** [27] was also synthesized from the condensation reaction of pyrene-1-carbaldehyde **10** and *o*-benzenediamine **12** in refluxing C_2H_5OH, which was used as a control compound for cation sensing studies.

A single crystal of **7** (CCDC: 2209686) suitable for X-ray analysis was obtained by slow evaporation of a $CHCl_3/CH_3CN$ = 5:1 solution. As shown in Fig. 1, a distorted 1,3-alternate conformation is observed, which is common for most oxa- [7,8] and aza-calix[4]arenes [9,10]. The two benzene rings with isobutylamino groups are almost parallel with a small dihedral angle of 11.85° and a centroid-centroid distance of 5.788 Å, while the two imidazobenzimidazole rings diverge with a large dihedral angle of 115.80° and a centroid-centroid distance of 6.725 Å. The two anthracenyls attached to the same imidazobenzimidazole are almost coplanar and vertical to the imidazobenzimidazole plane. An interesting packing mode was observed. They existed as dimers *via* off-set π-π stacking interactions (Fig. S13 in Supporting information) between imidazobenzimidazole rings (centroid-centroid distance: 3.541 Å) and anthracenyls (centroid-centroid distance: 5.500 Å and inter anthracenyl distance: about 3.4 Å). Each dimer further interacts with other four dimers *via* off-set π-π stacking interactions between the pendent anthracenyls (Fig. S14 in Supporting information).

A 1,3-alternate conformation was also found for the single crystal of **11** (CCDC: 2209690), which was obtained *via* slow evaporation of a THF/C_2H_5OH = 3:1 solution (Fig. 2a). The dihedral angles between benzene rings and imidazobenzimidazole rings are 38.98° and 124.63°, respectively. The centroid-centroid distances are 6.226 Å and 6.794 Å, respectively. The conformation is not so distorted as that for **7**. Two pyrenyls attached to one imidazobenzimidazole ring are almost on the same plane (with a dihedral angle of 8.54°) and perpendicular to the imidazobenzimidazole ring, while the other two pyrenyls on the other imidazobenzimidazole ring are a little twisted with a dihedral angle of 24.48° and extend toward opposite directions. **11** also existed as dimers in the solid state. But the intermolecular interactions are different. Three folds of off-set π-π stacking interactions between pyrenyls and imidazobenzimidazole rings, together with four folds edge-to-face T-shape π-π interactions [38,39] or CH-π hydrogen bonding [40] between pyrenyls (with centroid-centroid distances of 6.727 Å and 6.458 Å) account for the dimerization (Fig. 2b). Different to

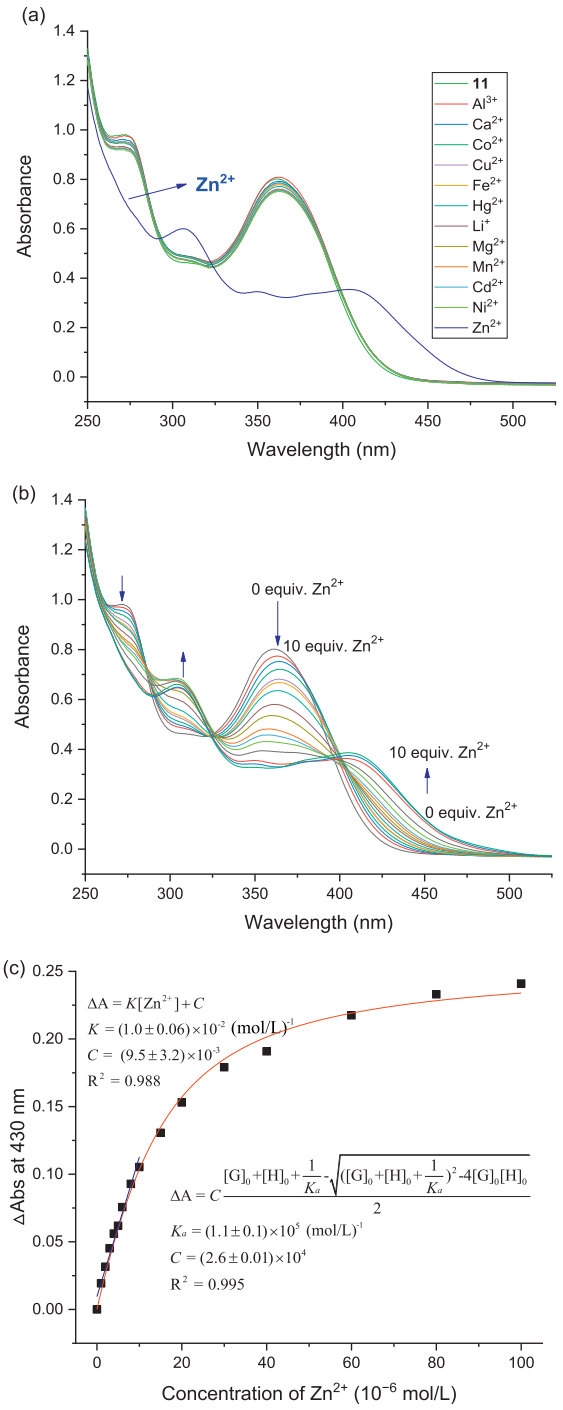

Fig. 3. (a) UV–vis absorption spectra of tetrapyrenyl modified compound **11** (1×10^{-5} mol/L in $CHCl_3$) upon addition of various metal ions (10 equiv.); (b) UV-vis titration curves of **11** (fixed at 1×10^{-5} mol/L in $CHCl_3$) with 0~10 equiv. of Zn^{2+} (bulk solution: 2×10^{-3} mol/L in CH_3CN), 298 K; (c) nonlinear fitting (red curve) of the absorption data at λ = 430 nm into a 1:1 binding mode to determine the association constant K_a for complex **11**–Zn^{2+}. The insets show the linear fitting result in the concentration range from 1×10^{-6} mol/L to 1×10^{-5} mol/L (blue line).

7, further packing of the dimers of **11** was dominated mainly by two folds of edge-to-face T-shape π-π interactions, with centroid-centroid distances of 6.794 Å and 7.616 Å, respectively (Fig. S16 in Supporting information).

We further tested the cation sensing ability of the fluorophores modified **7** and **11**. The cations were screened *via* fluorescence spectroscopy. When excited with λ_{ex} = 393 nm, more or less

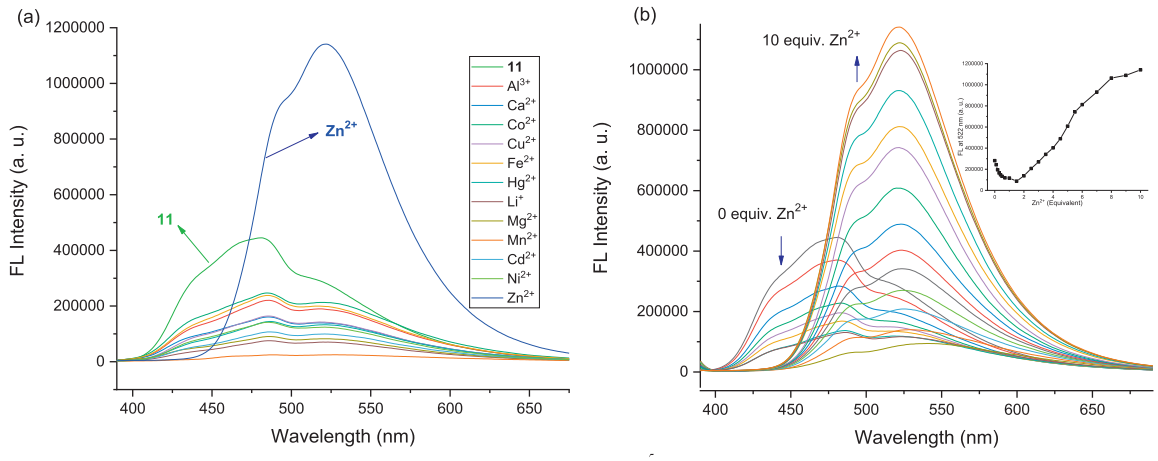

Fig. 4. (a) FL emission spectra of pyrenyl modified compound **11** (1×10^{-5} mol/L in $CHCl_3$) upon addition of various metal ions (10 equiv.), λ_{ex} = 381 nm; (b) FL titration curves of **11** (fixed at 1×10^{-5} mol/L in $CHCl_3$) with 0∼10 equiv. of Zn^{2+} (bulk solution: 2×10^{-3} mol/L in CH_3CN), 298 K. The insert shows FL intensity changes at λ = 522 nm with addition of 0∼10 equiv. of Zn^{2+}.

changes in fluorescence emission spectra were observed for the anthracenyl modified **7** (Fig. S17 in Supporting information) upon addition of different cations: it showed little selectivity. Upon mixing **11** with $Zn(ClO_4)_2$ in $CHCl_3$, the solution changed from colourless to light yellow. However, addition of ClO_4^- salts of other cations such as Al^{3+}, Ca^{2+}, Co^{2+}, Cu^{2+}, Fe^{2+}, Hg^{2+}, Li^+, Mg^{2+}, Mn^{2+}, Cd^{2+}, and Ni^{2+} led to negligible changes (Fig. S18a in Supporting information). UV-vis measurements (Fig. 3a) further revealed that new absorption bands at λ = 306 nm and λ = 420 nm appeared upon addition of 10 equiv. of Zn^{2+}. Addition of the above mentioned other cations only led to minor changes in the absorption bands at λ = 275 nm and λ = 361 nm. UV-vis titration studies (Fig. 3b) indicated that the absorption bands at λ = 275 nm and λ = 361 nm decreased and two new absorption bands at λ = 306 nm and λ = 420 nm evolved with gradual addition of Zn^{2+}. The titration curves showed two clear isosbestic points at λ = 322 nm and λ = 396 nm, indicating formation of a well-defined **11**–Zn^{2+} complex. Job's plot *via* UV-vis measurements by fixing the total concentration of **11** and Zn^{2+} at 1×10^{-5} mol/L revealed a 1:1 stoichiometry for the complex **11**–Zn^{2+} (Figs. S19 and S20 in Supporting information) [41]. Nonlinear fitting the above UV-vis titration data at λ = 430 nm into a 1:1 binding mode yielded an association constant K_a of 1.1×10^5 L/mol (Fig. 3c) for the complex **11**–Zn^{2+} [42]. In the concentration range from 1×10^{-6} mol/L to 1×10^{-5} mol/L, a good linear relationship (Fig. 3c, R^2 = 0.988) between ΔA and the concentration of Zn^{2+} was found.

The selective sensing ability of **11** toward Zn^{2+} was further investigated *via* FL measurements. **11** itself in $CHCl_3$ showed weak yellow fluorescence under λ = 365 nm UV lamp. With addition of 10 equiv. of Zn^{2+}, a bright yellow fluorescence was observed (Fig. S18b). However, addition of other cations did not lead to apparent changes. FL measurements revealed a remarkably strong emission band at λ = 522 nm and a shoulder band at λ = 500 nm upon addition of Zn^{2+} (Fig. 4a) when excited with λ_{ex} = 381 nm. **11** itself showed a modest emission band at λ = 481 nm and a shoulder band at λ = 520 nm. Addition of other cations led to partial quenching of the fluorescence. Titration curves (Fig. 4b) further revealed that the fluorescence was quenched with gradual addition of the first 1.5 equiv. of Zn^{2+}. With further addition of Zn^{2+}, the emission band at λ = 522 nm evolved. The limit of detection (LOD) was calculated to be 2.3×10^{-6} mol/L (Fig. S21 in Supporting information).

The selective sensing of Zn^{2+} showed strong anti-interference in the presence of other cations. Whatever addition of 10 equiv. of Zn^{2+} to a solution of compound **11** and other cations in $CHCl_3$, or addition of other cations to a solution of complex **11** and Zn^{2+}, similar changes in solution colour, UV-vis (Fig. S22 in Supporting information) and FL (Fig. S23 in Supporting information) spectra were observed as if other metal ions did not exist.

The sensing process is completely reversible as exemplified by alternate addition of Zn^{2+} and F^-. Addition of two equivalents of F^- to a solution of complex **11**–Zn^{2+} could restore the UV-vis absorption almost completely to the initial state and the solution colour faded. This process could be circulated several times by continuous alternate additions of Zn^{2+} and F^- (Figs. S24 and S25 in Supporting information).

Our sensor **11** is almost insoluble in water. Following a simple protocol developed by Cragg *et al.* [43], we showed that **11** could, in principle, be used to analyse Zn^{2+} in aqueous samples. A mixture of our sensor **11** and 2∼10 equiv. of $Zn(ClO_4)_2$ in 3 mL 1:1 $CHCl_3$-H_2O in a sealed tube was heated to reflux for 24 h. After evaporation of the solvent under reduced pressure, the residue was re-dissolved in 1:1 $CHCl_3$-CH_3CN and subjected to fluorescence measurements. A good linear relationship between the FL intensity at λ = 522 nm and the concentration of Zn^{2+} (Fig. S29 and Fig. S30 in Supporting information) was revealed.

However, with our control compound **13**, addition of all the above mentioned cations caused no apparent colour change (Fig. S26 in Supporting information), minor changes in UV-vis (Fig. S27 in Supporting information) and FL spectra (Fig. S28 in Supporting information). The high Zn^{2+}-selective sensing ability of **11** might come from cooperative action of four pre-organized N atoms on one rim, which captured the Zn^{2+} with an appropriate diameter. The conformation flexibility of the host itself might also account for the selective sensing process. Upon coordination with Zn^{2+}, the pyrenyls on different imidazobenzimidazole heterocycles were drawn close and oriented in a face-to-face manner, which might be the origin of the excimer emission.

In summary, imidazobenzimidazole fused aza-calix[4]arenes were synthesized by condensation reactions of a tetra(amino)-azacalix[4]arene and various aromatic aldehydes. For the first time, the bridging NH sites were involved in the functionalization of the aza-calix[4]arene framework. Various aromatic motifs including anthracenyl and pyrenyl fluorophores could be introduced. Distorted 1,3-alternate conformations were observed for the imidazobenzimidazole fused aza-calix[4]arenes in the solid state. They existed as unique dimers *via* multi-fold of π-π stacking interactions between planar fluorophores. The pyrenyl modified product

could be used as a colorimetric and "off-on" fluorometric sensor for Zn^{2+}. Job's plot *via* UV-vis measurements revealed a 1:1 stoichiometry and an association constant of 1.1×10^5 L/mol was determined. The selective sensing showed strong anti-interference in the presence of various other cations. The sensing process is completely reversible as proved *via* alternate addition of Zn^{2+} and F^-. Aza-calix[4]arene skeleton with relatively fixed but still adjustable conformation proved itself to be a good platform for fabricating fluorescent sensors.

Declaration of competing interest

The authors declare that they have no known competing financial interests or personal relationships that could have appeared to influence the work reported in this paper.

Acknowledgment

This work is supported by National Natural Science Foundation of China (Nos. 21971223 and 21772178).

Supplementary materials

Supplementary material associated with this article can be found, in the online version, at doi:10.1016/j.cclet.2023.108294.

References

[1] C.D. Gutsche, Calixarenes: An Introduction, 2nd Ed., RSC Pub., Cambridge, 2008.
[2] P. Neri, J.L. Sessler, M.X. Wang, Calixarenes and Beyond, Springer International Publishing, 2016.
[3] B. König, M.H. Fonseca, Eur. J. Inorg. Chem. (2000) 2303–2310.
[4] M.X. Wang, Acc. Chem. Res. 45 (2012) 182–195.
[5] N. Morohashi, F. Narumi, N. Iki, T. Hattori, S. Miyano, Chem. Rev. 106 (2006) 5291–5316.
[6] R. Kumar, Y.O. Lee, V. Bhalla, M. Kumar, J.S. Kim, Chem. Soc. Rev. 43 (2014) 4824–4870.
[7] W. Maes, W. Dehaen, Chem. Soc. Rev. 37 (2008) 2393–2402.
[8] R. Hudson, J.L. Katz, Oxacalixarenes, in: P. Neri, J.L. Sessler, M.X. Wang (Eds.), Calixarenes and Beyond, Springer International Publishing, 2016, pp. 399–420.
[9] D.X. Wang, M.X. Wang, Azacalixaromatics, in: P. Neri, J.L. Sessler, M.X. Wang (Eds.), Calixarenes and Beyond, Springer International Publishing, 2016, pp. 363–398.
[10] H. Tsue, K. Ishibashi, R. Tamura, Top. Heterocycl. Chem. 17 (2008) 73–96.
[11] N. Sommer, H.A. Staab, Tetrahedron Lett. 7 (1966) 2837–2841.
[12] G.W. Smith, Nature 198 (1963) 879.
[13] M.X. Wang, H.B. Yang, J. Am. Chem. Soc. 126 (2004) 15412–15422.
[14] J.L. Katz, M.B. Feldman, R.R. Conry, Org. Lett. 7 (2005) 91–94.
[15] J.L. Katz, K.J. Selby, R.R. Conry, Org. Lett. 7 (2005) 3505–3507.
[16] N. Kumar, P.X. Qui, I.Leray Roopa, M.H. Ha-Thi, Calixarene-based fluorescent molecular sensors, in: J.L. Atwood (Ed.), Comprehensive Supramolecular Chemistry II, Elsevier B.V., 2017, pp. 197–226.
[17] R. Kumar, A. Sharma, H. Singh, et al., Chem. Rev. 119 (2019) 9657–9721.
[18] A. Peterson, M.L. Ludvig, J. Martonova, et al., Supramol. Chem. 32 (2020) 313–319.
[19] V. Mehta, M. Athar, P.C. Jha, et al., New J. Chem. 41 (2017) 5125–5132.
[20] H.X. Wang, Z. Meng, J.F. Xiang, et al., Chem. Sci. 7 (2016) 469–474.
[21] M. Panchal, M. Athar, P.C. Jha, et al., RSC Adv. 6 (2016) 53573–53577.
[22] G. Canard, J.A. Edzang, Z. Chen, et al., Chem. Eur. J. 22 (2016) 5756–5766.
[23] Y. Bansal, O. Silakari, Bioorg. Med. Chem. 20 (2012) 6208–6236.
[24] S. Choudhary, M. Arora, H. Verma, M. Kumar, O. Silakari, Eur. J. Pharmacol. 899 (2021) 174027.
[25] M. Sweeney, D. Conboy, S.I. Mirallai, F. Aldabbagh, Molecules 26 (2021) 2684.
[26] Z. Xu, N.J. Singh, S.K. Kim, et al., Chem. Eur. J. 17 (2011) 1163–1170.
[27] A. Kushwaha, S.K. Patil, D. Das, New J. Chem. 42 (2018) 9200–9208.
[28] A.L. Brazeau, K. Yuan, S.B. Ko, I. Wyman, S. Wang, ACS Omega 2 (2017) 8625–8632.
[29] N. Kaur, G. Dhaka, J. Singh, New J. Chem. 39 (2015) 6125–6129.
[30] M. Barwiolek, A. Wojtczak, A. Kozakiewicz, et al., New J. Chem. 42 (2018) 18559–18568.
[31] P. Guo, A.A. Farahat, A. Paul, D.W. Boykin, W.D. Wilson, Chem. Sci. 12 (2021) 15849–15861.
[32] S.G. Wang, Y. Pang, M. Xue, Y. Yang, New J. Chem. 45 (2021) 19219–19223.
[33] J.B. Birks, Rep. Prog. Phys. 38 (1975) 903–974.
[34] F.M. Winnik, Chem. Rev. 93 (1993) 587–614.
[35] L. Lavaud, S. Pascal, K. Metwally, et al., Chem. Commun. 54 (2018) 12365–12368.
[36] Z. Chen, R. Haddoub, J. Mahe, et al., Chem. Eur. J. 22 (2016) 17820–17832.
[37] A.A. Farahat, S. Iwamoto, M. Roche, D.W. Boykin, J. Heterocycl. Chem. 58 (2021) 2280–2286.
[38] C.A. Hunter, J.K.M. Sanders, J. Am. Chem. Soc. 112 (1990) 5525–5534.
[39] R. Thakuria, N.K. Nath, B.K. Saha, Cryst. Growth Des. 19 (2019) 523–528.
[40] M. Nishio, CrystEngComm 6 (2004) 130.
[41] J. Polster, H. Lachmann, Spectrometric Titrations: Analysis of Chemical Equilibria, Wiley-VCH, 1989.
[42] P. Thordarson, Chem. Soc. Rev. 40 (2011) 1305–1323.
[43] E. Manandhar, P.J. Cragg, K.J. Wallace, Supramol. Chem. 26 (2014) 141–150.